Ultrasound in Med. & Biol., Vol. 35, No. 2, pp. 256–265, 2009

0301-5629/09/$–see front matter

ELSEVIER

doi:10.1016/j.ultrasmedbio.2008.08.012

● *Original Contribution*

REGION-BASED ENDOCARDIUM TRACKING ON REAL-TIME THREE-DIMENSIONAL ULTRASOUND

Qi Duan,* Elsa D. Angelini,† Susan L. Herz,* Christopher M. Ingrassia,* Kevin D. Costa,* Jeffrey W. Holmes,* Shunichi Homma,* Andrew F. Laine*

*Department of Biomedical Engineering, Columbia University, New York, NY, USA; and †Department of Image and Signal Processing, Institut Telecom, Telecom ParisTech, Paris, France

(*Received* 2 *October* 2007; *revised* 30 *July* 2008; *in final form* 14 *August* 2008)

Abstract—Matrix-phased array transducers for real-time 3-D ultrasound enable fast, noninvasive visualization of cardiac ventricles. Typically, 3-D ultrasound images are semiautomatically segmented to extract the left ventricular endocardial surface at end-diastole and end-systole. Automatic segmentation and propagation of this surface throughout the entire cardiac cycle is a challenging and cumbersome task. If the position of the endocardial surface is provided at one or two time frames during the cardiac cycle, automated tracking of the surface over the remaining time frames could reduce the workload of cardiologists and optimize analysis of 3-D ultrasound data. In this paper, we applied a region-based tracking algorithm to track the endocardial surface between two reference frames that were manually segmented. To evaluate the tracking of the endocardium, the method was applied to 40 open-chest dog datasets with 484 frames in total. Ventricular geometry and volumes derived from region-based endocardial surfaces and manual tracing were quantitatively compared, showing strong correlation between the two approaches. Statistical analysis showed that the errors from tracking were within the range of interobserver variability of manual tracing. Moreover, our algorithm performed well on ischemia datasets, suggesting that the method is robust-to-abnormal wall motion. In conclusion, the proposed optical flow-based surface tracking method is very efficient and accurate, providing dynamic "interpolation" of segmented endocardial surfaces. (E-mail: qd2002@columbia.edu)

Key Words: **Real-time 3-D echocardiography, Optical flow, Speckle tracking, Quantitative evaluation, Open-chest ultrasound, LV, Endocardium.**

INTRODUCTION

Cardiac screening using ultrasound is beneficial because it provides the highest temporal resolution but is limited to two dimensions in most medical centers. Development of 3-D echocardiography began in the late 1980s with the introduction of off-line 3-D medical ultrasound imaging systems. Many review articles have been published over the past decade assessing the progress and limitations of 3-D ultrasound technology for clinical screening (Belohlavek et al. 1993; Fenster and Downey 2000; Ofili and Nanda 1994; Rankin et al. 1993). These articles reflect the diversity of 3-D systems developed for both image acquisition and reconstruction. Although 2-D transducers can be configured to assemble a 3-D image from a series of planar views, for truly real-time acquisition, only matrix phased array transducers can scan true 3-D volumes with stationary transducers (Ramm and Smith 1990). There are few alternative technologies that also enable real-time acquisition based on vibrating or fast rotating transducers (Canals et al. 1999; Voormolen et al. 2006). Real-time 3-D ultrasound technology is an improvement over former generations of 3-D systems because volumetric data can be acquired rapidly (20 to 25 frames per second), enabling cardiologists to visualize moving cardiac structures from any given plane in real-time. A first generation of real-time 3-D ultrasound (RT3D) scanners was introduced in the early 1990s by Volumetrics© (Ramm and Smith 1990), but low spatial resolution over the whole cardiac volume prevented the technology from meeting its initial expectation and reaching its full potential. A new generation of RT3D transducers was introduced by Philips Medical Systems (Best, The Netherlands) in the 2000s with the SONOS 7500, and most recently the iE33 ultrasound system,

Address correspondence to: Qi Duan, ET351, 1210 Amsterdam Avenue, New York, NY, 10025. E-mail: qd2002@columbia.edu

which can acquire a fully-sampled cardiac volume in four cardiac cycles. Four sector acquisitions are performed with each scan, acquiring 1/4 of the cardiac volume. These sectors are spatially aggregated to generate one ultrasound volume over one cardiac cycle. This technical design enabled dramatically increased spatial resolution and image quality. The latest research upgrade of iE33 also enables a true real-time model, which provides 4-D ultrasound streaming data without any spatial compounding (Duan et al. 2007b).

Clinical evaluation of 3-D ultrasound data for assessment of cardiac function is performed *via* visualization using selected 2-D projection planes. Inspection of 3-D datasets with 2-D visualization tools is time-demanding, motivating the development of computational tools for quantitative analysis of ventricular function. It has been shown that abnormal ventricular wall motion can be detected accurately on RT3D data, with quantitative four-dimensional analysis of the endocardial surface and computation of local fractional shortening (Herz et al. 2005; Ingrassia et al. 2007). Monaghan's group has also shown that endocardial surface data derived from RT3D ultrasound is valuable in accessing dyssynchrony (Horstman et al. 2007; Kapetanakis et al. 2005). These preliminary studies confirmed that RT3D ultrasound provides unique and valuable quantitative information about cardiac motion based on manually or semiautomatically traced endocardial contours. To facilitate the segmentation process over the entire cardiac cycle, we evaluated the use of region-based tracking between segmented frames to alleviate the manual tracing task. In previous research on motion tracking with ultrasound data, intensity-based optical flow (OF) tracking methods described previously (Bardinet et al. 1996; Boukerroui et al. 2003; Mikic et al. 1998; Paragios 2003; Tsuruoka et al. 1996; Yu et al. 2003) combined local intensity correlation with specific regularizing constraints (*e.g.*, continuity of the displacements). The presence of speckle noise in ultrasound prevents the use of gradient-based methods; however relatively large region-matching methods are robust to the presence of noise. In this study, we propose a surface tracking application using a 4-D correlation-based tracking method on 3-D volumetric ultrasound intensity data.

This study aimed to address the following questions, focusing on the left ventricle (LV):

1. Can the proposed method track the endocardial surface between end-diastole (ED) and end-systole (ES) with reliable positioning accuracy?
2. How does dynamic information derived from tracking on RT3D ultrasound compare with information obtained from a single segmentation method?
3. Can the proposed method be used as a dynamic interpolation tool for tracking the endocardial surface?

METHODS

Region-based tracking using correlation metric

When Horn and Schunck (1981) proposed the term "optical flow," it was defined as "the distribution of apparent velocities of movement of brightness patterns in an image." In other words, the original optical flow definition was referring to a velocity field or displacement field of the motion of pixel patterns in an image. Optical flow tracking involves the computation of such fields on deforming objects in an image, based on the assumption that the intensity of the object remains constant over time. In this context, object motion is characterized by a flow of pixels with constant intensity. There are two widely used families of OF computation techniques (Barron et al. 1994): (i) differential techniques (Cremers et al. 2007; Frangi et al. 2001; Horn and Schunck 1981; Lucas and Kanade 1981a; Nagel 1983; Yilmaz et al. 2006) that compute velocity from spatio-temporal derivatives of pixel intensities based on the "optical flow constraint" equation: $I_x v_x + I_y v_y + I_z v_z + I_t = 0$ with spatial-temporal gradients I_* of image I and spatial components of optical flow vector v_* (Black and Anandan 1996; Horn and Schunck 1981b; Lucas and Kanade 1981b); and (ii) region-based matching techniques (Anandan 1989; Singh 1990), which compute OF by identifying local displacements that correlate best between two consecutive image frames. Because the first two pilot studies on optical flow estimation (Horn and Schunck 1981; Lucas and Kanade 1981b) were focused on differential techniques, differential OF accounts for a large portion of OF-based applications (Ledesma-Carbayo et al. 2005; Suhling et al. 2005; Veronesi et al. 2006). Compared with differential OF approaches, region-based methods use similarity measures, such as summed-squared differences or cross-correlation coefficients that are less sensitive to noise, fast motion and potential occlusions and discontinuities (Anandan 1989; Bleyer et al. 2005; Convertino 1997; Linguraru et al. 2006; Revell et al. 2004; Singh 1990; Wang et al. 2007; Xiao et al. 2005), while assuming that displacements in small neighborhoods are similar. Given the relatively high noise corrupting 3-D ultrasound volume series, we adopted a region-based tracking approach to estimate myocardial surface displacements between two consecutive frames. Specifically, we used a correlation metric-based tracking method.

Given two datasets from consecutive time frames: $(I(x,t), I(x,t + \Delta t))$, the displacement vector Δx for pixels in a small neighborhood Ω around each pixel x is esti-

mated by maximizing the cross-correlation coefficient as follows:

$$r = \frac{\sum_{x\varepsilon\Omega} \left(I(x,t)I(\mathrm{x}+\Delta\mathrm{x},t+\Delta t)\right)}{\sqrt{\sum_{\mathrm{x}\varepsilon\Omega} I^2(\mathrm{x},t)\sum_{\mathrm{x}\varepsilon\Omega} I^2(\mathrm{x}+\Delta\mathrm{x},t+\Delta t)}}. \quad (1)$$

In this study, correlation-based tracking was performed in 3-D to estimate the displacement of selected voxels between two consecutive ultrasound volumes in the cardiac cycle. The search window Ω was centered around every ($5 \times 5 \times 5$) pixel volume and was set to size ($7 \times 7 \times 7$) for a voxel size of $0.6 \times 0.6 \times 0.6$ mm. Regularization of the displacement field was enforced *via* local averaging of the vector values. *A priori* information on high contrast between the myocardium and the blood was incorporated in the tracking process to avoid tracking in blood region and minimize erroneous tracking positions, falling away from the endocardial surfaces. Preprocessing of the RT3D data with a speckle-specific anisotropic diffusion filter previously designed by our group (Duan et al. 2004) was applied before the tracking.

Preprocessing

Because noise in the data will degrade the performance in motion-tracking algorithms (Bachner et al. 2007; Yu et al. 2006), all datasets were presmoothed with edge-preserving anisotropic diffusion as developed in Duan et al. (2004). Anisotropic diffusion methods apply the following heat-diffusion dynamic equation to the gray levels of a given 3-D image dataset I (x,y,z,t):

$$\frac{\partial I}{\partial t} = div(c(x,y,z,t)\nabla I), \quad (2)$$

where c (x, y, z, t) is the diffusion parameter, div denotes the divergence operator and ∇I is the gradient of the image intensity.

In the original work of Perona and Malik (1987, 1990), the concept of anisotropic diffusion was introduced with the selection of a variable diffusion parameter, which is a decreasing function *g* of the gradient of the image data:

$$c(x,y,z,t) = g(|\nabla I(x,y,z,t)|), \quad (3)$$

We used the diffusion function proposed by Weickert et al. (1998) defined as:

$$g(x,\lambda) = \begin{cases} 1 & x \le 0 \\ 1 - e^{\frac{3.315}{(x/\lambda)^4}} & x > 0 \end{cases}. \quad (4)$$

The parameter λ serves as a gradient threshold, defining edge points x_k at locations where $|\nabla I_{x_k}| > \lambda$. This bell-shaped diffusion function acts as an edge-enhancing filter, with high diffusion values in smooth areas and low values at edge points. The structure of the diffusion tensor with separate weights for each dimension enables to control the direction of the diffusion process, with flows parallel to edge contours.

In the case of noisy textured data, as ultrasound data with speckle noise, as the diffusion process evolves, the characteristics of the image data change and the gradient threshold parameter value should therefore be modified. It was reported in a paper by Montagnat et al. (2003) that values of significant edges decrease as homogeneous regions in the ultrasound data are filtered. Therefore, they chose to decrease the threshold gradient over time. Values were selected as a fraction of the cumulative histograms of the data gradients that were recomputed at each iteration of the diffusion process. In the proposed method, a linear model was used to control the gradient weight:

$$\lambda(t) = \lambda_0 + at, \quad (5)$$

with λ_0 representing an initial gradient value, a the slope parameter and *t* the time iteration index. Parameters were set empirically for the datasets processed. In our previous algorithm using Volumetrics© data (Duan et al. 2004), a linearly increasing scheme was used to suppress the granularity in the acquired images, whereas with the data acquired by the iE33 imaging system, such an aggressive diffusion process was not needed. In this paper, a decreasing scheme was used with $\lambda_0 = 20$ and a=-1. Sample cross-section views after denoising are shown in Fig. 1d–f.

Three-dimensional ultrasound datasets

The OF tracking approach was tested on 40 datasets, with 484 frames in total acquired with an iE33 3-D ultrasound machine. These data were obtained as part of a separate study under a protocol approved by Columbia University's Institutional Animal Care and Use Committee. Four coronary artery occlusions were performed on five anesthetized, open-chest dogs (20 occlusions total). Three-dimensional echocardiograms were acquired at baseline and 60–90 s after temporary ligation of the left anterior descending (LAD) and left circumflex (LCx) coronary arteries at the proximal and distal levels. These datasets were obtained by positioning the transducer directly on the apex of the heart, providing high image quality in a small field-of-view. Spatial resolution of the analyzed data was about $(0.6\ \mathrm{mm})^3$, and 10–14 frames were acquired during each cardiac cycle depending on the heart rate, under an acquisition frame rate of 20–25 frames per second. Cross-sectional views from one of the open-chest baseline datasets at end-diastole (ED) are shown in Fig. 1a–c. The data acquisition was gated by

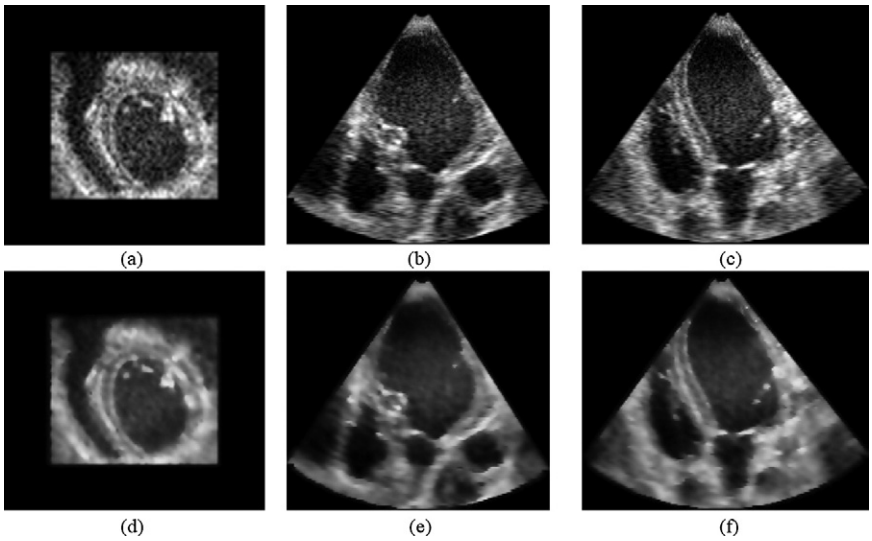

Fig. 1. Cross-sectional views at ED for one of the datasets. (a–c) Original data and (d–f) the data after diffusion process. (a, d) Axial; (b, e) elevation; and (c, f) azimuth views.

electrocardiogram (ECG) and the ED frame was the first frame for all 4-D data series.

Segmentation

The endocardial surface of the LV was semiautomatically segmented using TomTec© software (TomTec Inc., Munich, Germany). Manual editing of the endocardial surface was required. An experienced user performed manual tracing of all time frames on all datasets, on rotating B-scan views (long-axis views rotating around the central axis of the ventricle) and C-scan views (short-axis views at different depths).

Defining a "gold standard" for evaluating the performance of tracking is a challenging task. To evaluate segmentation or boundary extraction methods on clinical data are difficult in general because no ground truth can be perfectly defined. As a result, under such circumstances, segmentations from experienced users are typically regarded as the "ground truth." To take manual tracing variability into account, discrepancy of segmentation methods are usually compared with interobserver variability (Brandt et al. 1999; Heijman et al. 2008; Juergens et al. 2008; Pednekar et al. 2003; van Geuns et al. 2006), viewing the computer-based method as another "observer." If the discrepancy is comparable to interobserver variability, then it is safe to consider that the proposed method is acceptable because the error in the method has fallen within the variance of the ground truth. Following the same rationale, two additional trained cardiologists traced a subset of the data to measure interobserver variability. We hypothesized that region-based tracking of the endocardial surface from RT3D ultrasound data could achieve comparable accuracy to human observers' variability. In other words, we expected that surface discrepancy between a tracked surface and the corresponding manual tracing should be similar to the difference between two surfaces traced by two different trained users (or cardiologists), *i.e.*, the interobserver variability.

Tracking with region-based technique

Tracking of the endocardial surface was applied after initialization with manually traced ED data. Starting with a set of endocardial surface data (about 650 data points, roughly 1.5 mm apart) defined at ED, the tracking algorithm was used to track the surface in time throughout the entire cardiac cycle. The proposed method was not being applied as a segmentation tool, but used as a surface-tracking tool for a given segmentation method. No additional reinitialization or forward-and-backward tracking as proposed in Duan et al. (2005b) was needed because of high image quality provided by the open-chest acquisition setup.

Evaluation

We evaluated tracking accuracy by quantitatively comparing the dynamic ventricular geometry to the manually segmented surfaces. Segmentation results were typically compared using global measurements such as volume or mean-square errors. To provide regional comparisons, we proposed a novel comparison method based on a parameterization of the endocardial surface in prolate spheroidal coordinates (Ingrassia et al. 2003), which has been used previously for comparison of ventricular geometry from two 3-D ultrasound machines (Angelini et al. 2002). The endocardial surfaces were registered

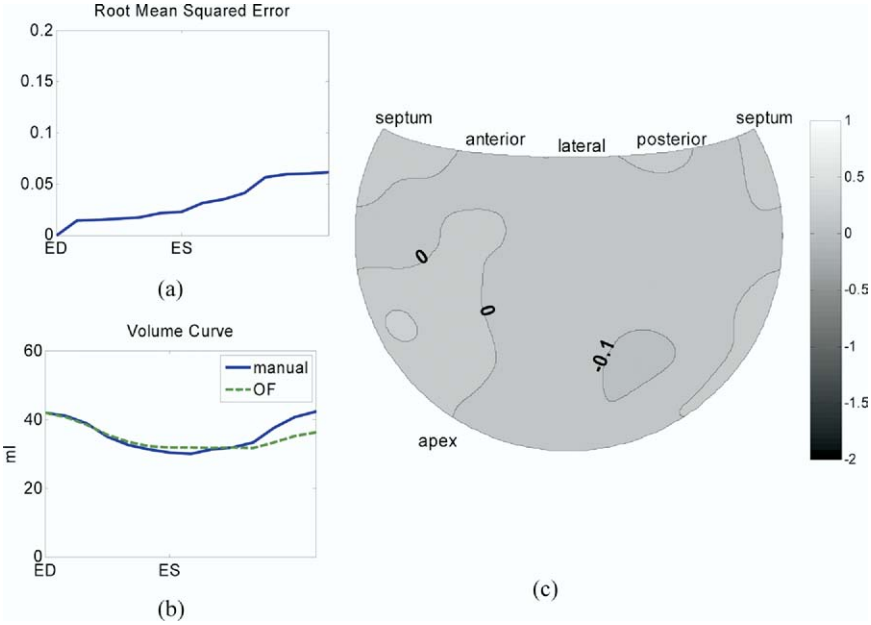

Fig. 2. (a-c) Example results fom one dataset. (a) Root-mean-square error (RMSE) of absolute differences in λ over one cardiac cycle; (b) LV volumes from manual tracing (solid line) and OF tracking (dashed line) over one cardiac cycle; and (c) relative difference maps between OF and manual tracing surfaces at ES, showing most of the surface under 10% (*i.e.*, 0.1) difference.

through time using three manually selected anatomical landmarks: the center of the mitral orifice, the endocardial apex and the equatorial midseptum point. The surface data were fitted in prolate spheroidal coordinates (λ,μ,θ), projecting the radial coordinate λ to a 64-element surface mesh with bicubic Hermite interpolation, yielding a realistic 3-D endocardial surface. The fitting process was performed using a custom finite element algorithm.

Fitted nodal values and spatial derivatives of the radial coordinate, λ, were then used to map relative differences between the two compared surfaces (*seg* from manual tracing and *RT* from region-based tracking), $\varepsilon = (\lambda_{seg} - \lambda_{RT}) / \lambda_{seg}$ using our custom software. Hammer mapping was used to preserve relative areas of the flattened endocardial surfaces (Hunter and Smaill 1988).

rms errors (RMSE) of the difference in λ, across the entire endocardial surface were computed for every time frame, between algorithm-tracked and the manual segmentation results. Because RMSE is actually the normalized distance between two surfaces, it could provide a fairer comparison than conventional point-to-surface metrics under clinical settings. Furthermore, it can be shown that multiplying the focus length of the model with the RMSE measurements will provide an upper bound of the point-wise errors. In other words, RMSE is a more conservative, efficient and clinically relevant version of the conventional metrics. Ventricular volumes were also computed for the manually segmented and the automatically tracked endocardial surfaces. Finally, relative λ difference maps were generated at end systole (ES), providing a direct quantitative comparison of ventricular geometry. These maps were visualized with isocontour lines, representing the fractional difference in λ position between the two surfaces.

RESULTS

Overall performance

As mentioned in the previous section, the regional-based tracking algorithm was initialized by manual tracing of the first frame (ED frame) for each of the 40 datasets. Then the endocardium was automatically tracked throughout the entire cardiac cycle, which provided 444 frames in total, where endocardial surface from both manual tracing and automated tracking were available. A sample result from one dataset is shown in Fig. 2. The time course of RMSE for this dataset is graphed in Fig. 2a, which shows small absolute errors ($<0.07 \sim 7\%$) despite error accumulation, as previously observed in Duan et al. (2005b). Time courses of the LV volumes estimated from manual tracing (solid line) and tracking (dashed line) are shown in Fig. 2b. These two measures were very close, especially during the systolic phase, except for the last two to three frames where accumulated errors became larger. Hammer mapping of the percent relative surface discrepancy at ES is shown in

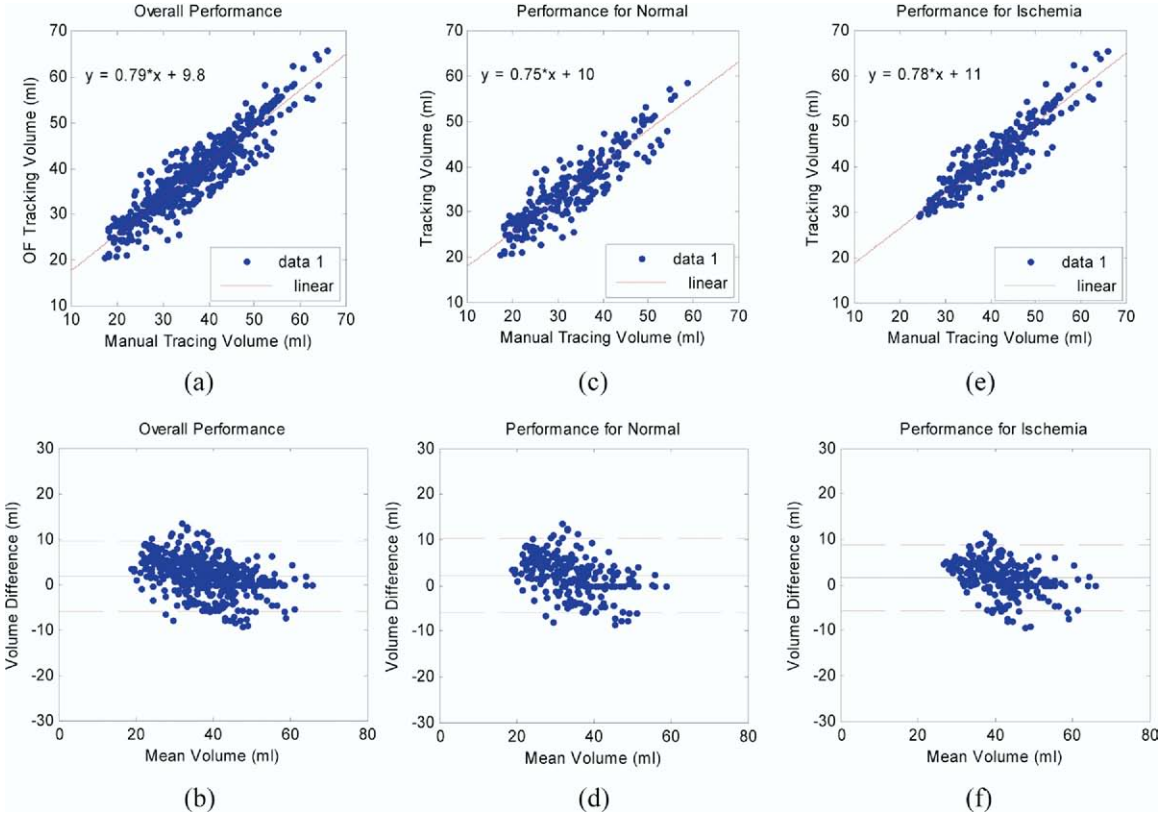

Fig. 3. Volume comparisons between manual tracing and region-based tracking. (a, b) Overall performance with regression plot (a) and Bland-Altman statistical analysis (b); (c, d) performance on normal group with regression plot (c) and Bland-Altman statistical analysis (d); and (e, f) performance on ischemia group with regression plot (e) and Bland-Altman statistical analysis (f). Each blue circle represents a single data point, the center black line represents the mean value and the two red dashed lines represent 95% confidence interval.

Fig. 2c. For this dataset, 96.7% of the entire endocardial surface generated from algorithm tracking had $<10\%$ difference when compared with the manually traced surface.

Across all 444 frames, the mean value of the RMSE was 0.05, with a standard deviation of 0.023540. The maximum RMSE value was 0.14. Regarding volume measurements, the mean difference in estimated volume for all 444 frames was 3.93 mL, with a standard deviation of 2.54 mL. The maximum difference in volume estimation was 13.59 mL. There was a strong correlation between volume measurements from region-based tracking and manual tracing, with a correlation coefficient $r = 0.93$ ($r^2 = 0.86$) and a slope of 0.79, with a bias of 9.8 mL. The regression plot and corresponding Bland-Altman plot are shown in Fig. 3a and b. Average computational time for tracking each frame was 9 s, with a standard deviation of 0.12 s and a maximum value of 9.2 s. All computations were implemented in C programming language and executed on a 2.4-GHz 64-bit AMD single processor server, running Red Hat Linux Enterprise AS.

Comparison to interobserver variability

Because it is difficult to define an absolute "gold standard" for the position of the endocardium, we used an alternate approach to validate our method. Our hypothesis is that region-based tracking of the endocardium from RT3D ultrasound can achieve comparable accuracy to human observer variability. We tested whether the difference between an algorithm-tracked surface and the corresponding manual tracing was comparable to the difference between two surfaces traced by separate experienced users, *i.e.*, interobserver variability.

To quantify interobserver variability, 12 datasets were randomly selected from the total 40 datasets. The ED frame for each dataset was traced by two cardiologists using separate customized software. All traced surfaces were reconstructed using the methods described above, and differences in surface positions and LV volumes were measured at ED. The reference tracings were similar to those used in the previous section.

On all 12 datasets, the mean value of the RMSE between the two cardiologists was 0.15, with a standard deviation of 0.14. The maximum RMSE value was 0.59.

Table 1. Statistics of surface discrepancies and volume differences for the normal group and the ischemia group

	Normal group	Ischemia group
Mean RMSE	0.06	0.05
STD RMSE	0.03	0.02
Max RMSE	0.14	0.10
Mean volume difference (mL)	4.24	3.61
STD volume difference (mL)	2.65	2.38
Max volume difference (mL)	13.59	11.48

The mean difference in estimated volumes for all frames was 11.83 mL, with a standard deviation of 9.64 mL. The maximum difference in volume estimation was 27.84 mL.

Region-based tracking provided smaller mean and standard deviation values for both RMSE and volume differences. Maximum RMSE and volume error values from region-based tracking were comparable to mean interobserver volume differences. To test the hypothesis that the performance of region-based tracking was comparable to interobserver errors, RMSE values between region-based tracking and manual tracing were compared with RMSE values between two experienced users' tracing by a two-sample *t*-test. Because our hypothesis is that region-based tracking has comparable performance with human expert tracing in terms of RMSE values, the null hypothesis for the statistical test was that RMSE values from region-based tracking had larger mean value than mean RMSE value from a human expert (a left-tail test), *i.e.*, region-based tracking had *worse* performance than an expert. Variances for both methods were not assumed equal for the purpose of fairness. The *t*-test with $\alpha = 0.05$ yielded a result of rejecting the null-hypothesis, with a *p*-value of 0.018, which indicates that statistically, region-based tracking is unlikely to have worse performance than manual tracing by multiple experts.

Performance comparison on baseline versus occlusion

To test the performance of region-based tracking on diseased cases with altered wall motion, we compared the ability of region-based tracking to track the endocardium on baseline datasets and during regional ischemia. It is clinically essential that computer-aided diagnostic tools perform well on abnormal data, which is not often addressed or tested in clinical studies evaluating the performance of such tools.

The recorded 444 data frames were divided into two groups: a normal group (224 frames) and an ischemia group (220 frames). Statistics on surface discrepancies and volume differences for each group are reported in Table 1.

To evaluate the difference in mean values of RMSE and volumes for each group, two-sample t-tests with $\alpha = 0.05$ were performed on RMSE values and volume differences. Abnormal data showed significantly lower RMSE and volume differences than normal data ($p =$ 5.97e-14 and 0.0085, respectively). An additional statistical power analysis yielded 100% power for RMSE values and 75.22% power for volume differences to detect the difference in the discrepancy measurement between the two groups with a two-sided *t*-test with type I error level of 0.05. These results suggest that our method may be valuable for clinical applications where abnormal wall motion may be present.

Results of regression plots and Bland-Altman plots for LV volume measures for the normal and ischemia groups were plotted in Fig. 3c–f. The 95% confidence interval is defined with a center value equal to the mean error and width equal to 2 standard deviations of the volume errors. These error intervals were equal to 2.55 mL $\pm$ 8.62 mL for normal group and 1.85 mL $\pm$ 7.83 mL for the ischemia group.

To best summarize the results for the volume comparisons between the overall manual and OF tracings, the interobserver results and the two comparisons between manual and OF tracings for the normal and ischemia subgroups, five metrics for each study including regression equation, correlation, standard error of the estimate, mean difference and limit of agreement and *p*-value of the *t*-test, are presented in Table 2.

DISCUSSION

Based on the presented quantitative validation studies, results on comparison between OF tracking and

Table 2. Correlation measures and statistical differences: Volume comparisons between the overall manual tracing and region-based tracking, inter-observer variability and comparisons between manual tracing and region-based tracking for the normal and ischemia subgroups

Study	Regression equation	Correlation	Standard error of the estimate	Mean difference	*p*-value
Overall	$y = 0.79x + 9.81$	0.93	3.23	10.88	0.001
Interobserver	$y = 1.23x - 3.70$	0.54	12.96	15.78	0.16
Normal	$y = 0.75x + 10.48$	0.91	3.30	10.26	0.005
Ischemia	$y = 0.78x + 10.93$	0.92	3.03	9.65	0.034

manual tracing were very encouraging. A strong correlation pattern between manual tracing and region-based tracking was found with correlation coefficients as well as the slope and the bias values comparable to findings in the literature (Angelini et al. 2005; Corsi et al. 2001; Sanchez-Ortiz et al. 2002) on RT3D ultrasound segmentation.

Tracking errors were within the range of interobserver variability, which were confirmed by statistical tests. Although the mean values of RMSE and volume differences from region-based tracking were smaller than from two experienced users, it cannot be inferred that region-based tracking had better performance. One reason that the errors for the proposed method were lower was that the region-based tracking was initialized by the user to whom the tracing was compared. If tracking errors were within the range of interobserver variability, it is nonetheless safe to conclude that, when initialized using manual tracing of the ED frame, region-based tracking is a good alternative to tracing every time frame in a RT3D ultrasound study.

The reason that region-based tracking performed better in the ischemia data compared with the normal data were probably related to the reduced motion caused by ischemia, which made tracking easier. However, this is an important feature compared with shape-based segmentation algorithms, for which abnormal wall motion sometimes generates abnormal shapes that would complicate the segmentation process.

Minimal computational time was required for analysis, with region-based tracking requiring <2 min to track the endocardial surface over the entire cardiac cycle compared with the time required for manual tracing by a cardiologist (1 h). This computational time is reasonable for processing RT3D ultrasound datasets in a clinical setting. Although measurements of fractional shortening or ejection fraction require only ED and ES time frames, region-based tracking may be particularly useful for LV synchrony analysis, which requires the segmentation of the entire cardiac cycle.

Although current RT3D ultrasound can offer 20–25 frames per second, as reported in the acquisition setup of the data used in this paper, the actual number of frames per cardiac cycle is limited by the heart rate as well. In most clinical settings, RT3D ultrasound usually can provide 16–20 frames per cardiac cycle. Under animal experiments, especially during some depressed situations such as open-chest experiments, the heart rate increases to 110–130 bpm on average so that actual frames available in one cardiac cycle become limited. Moreover, current 3-D technology cannot reach a frame rate above 100 frames per second, as in 2-D echocardiography. These screening constraints remain limiting factors in the application of RT3D ultrasound for motion analysis. However, this limitation is not an intrinsic limitation for the region-based tracking, but rather a limitation of current RT3D ultrasound technology. Region-based tracking can work with higher frame rate as well. As the advances of RT3D ultrasound technology, the performance of the proposed framework will also be expected to improve given the higher temporal resolution of the data.

As pointed out in Bland and Altman (1986), regression analysis alone is not sufficient to validate the performance of novel clinical measurements such as region-based tracking of the endocardium. For this reason, statistical analyses including *t*-test and power analysis were also included in the evaluation of our method, which all yielded consistent results.

Lastly, this study was focused on validating the tracking ability of the region-based tracking algorithm. The displacement field, a by-product of the tracking, also provided novel 4-D dynamic cardiac information that may be useful for analyzing RT3D ultrasound data. Detailed discussion on this extension of the method can be found in Duan et al. (2005a, 2006, 2007a).

CONCLUSION

A correlation-based tracking method was evaluated for its ability to track the LV endocardial surface over the entire cardiac cycle in RT3D ultrasound after being initialized with manual segmentation of the ED frame. Endocardial surface geometries obtained from manual segmentation and region-based tracking were compared at every time frame in the cardiac cycle. This geometric comparison was mapped and results were promising, showing that region-based tracking closely followed the endocardial surface throughout the entire cardiac cycle on 444 data frames. There was a strong correlation between region-based tracking and manual tracing. Statistical analysis showed that tracking errors were within the range of interobserver variability, with manual tracing by expert cardiologists. Moreover, our algorithm performed well both on normal and ischemia data, suggesting that our method may be valuable for clinical applications where abnormal wall motion may be present. This study showed that region-based tracking can accurately track the LV endocardial surface, yielding dynamic information from RT3D ultrasound data, and provides automated dynamic interpolation between segmented endocardial surfaces.

Acknowledgments—This work was partially funded by the National Science Foundation grant BES-02-01617, the American Heart Association grant #0151250T and #0640005N, Philips Medical Healthcare and the New York State NYSTAR/CAT Technology Program. The authors also would like to thank Dr. Jie Wang (The Skirball Animal Center, Orangeburg, NY) for helping with the animal experiments.

REFERENCES

Anandan P. A computational framework and an algorithm for the measurement of visual motion. Int J Comp Vision 1989;2:283–310.

Angelini E, Homma S, Pearson G, Holmes J, Laine A. Segmentation of real-time three-dimensional ultrasound for quantification of ventricular function: A clinical study on right and left ventricles. Ultrasound Med Biol 2005;31:1143–1158.

Angelini ED, Hamming D, Homma S, Holmes J, Laine A. Comparison of segmentation methods for analysis of endocardial wall motion with real-time three-dimensional ultrasound. Comp Cardiol 2002; 00:609–612.

Bachner N, Adam D, Leitman M, Vered Z. Ultrasound echocardiographic assessment of transmural inhomogeneity of the left ventricular contraction during the heart cycle. Comp Cardiol 2007;34: 817–820.

Bardinet E, Cohen LD, Ayache N. Tracking and motion analysis of the left ventricle with deformable superquadratics. Med Image Anal 1996;1:129–149.

Barron JL, Fleet D, Beauchemin S. Performance of optical flow techniques. Int J Comp Vision 1994;12:43–77.

Belohlavek M, Foley DA, Gerber TC, Kinter TM, Greenleaf JF, Seward JB. Three- and four-dimensional cardiovascular ultrasound imaging: A new era for echocardiography. Mayo Clin Proc 1993; 68:221–240.

Black MJ, Anandan P. The robust estimation of multiple motions: Parameteric and piecewise-smooth flow fields. Comp Vision Image Understanding 1996;63.

Bland J, Altman D. Statistical methods for assessing agreement between two methods of clinical measurement. Lancet 1986;i:307–310.

Bleyer M, Gelautz M, Rhemann C. Region-based optical flow estimation with treatment of occlusions. Joint Hungarian-Austrian Conference on Image Processing and Pattern Recognition 2005;235–242.

Boukerroui D, Noble JA, Brady M. Velocity estimation in ultrasound images: A block matching approach. Lecture Notes Comp Sci 2003;edn2732:586–598.

Brandt E, Wigstrom L, Wranne B. Segmentation of echocardiographic image sequences using spatio-temporal information. Lecture Notes Comp Sci 1999;1679:410–419.

Canals R, Lamarque G, Chatain P. Volumetric ultrasound system for left ventricle motion imaging. IEEE Trans Ultrason Ferroelectr Freq Control 1999;46:1527–1538.

Convertino G. Region-based optical flow estimation technique for collision avoidance. SPIE—Intelligent Robots and Computer Vision XVI: Algorithms, Techniques, Active Vision, and Materials Handling. 1997:118–125.

Corsi C, Borsari M, Consegnati F, Sarti A, Lamberti C, Travaglini A, Shiota T, Thomas JD. Left ventricular endocardial surface detection based on real-time 3D echocardiographic data. Eur J Ultrasound 2001;13:41–51.

Cremers D, Rousson M, Deriche R. A review of statistical approaches to level set segmentation: Integrating color, texture, motion and shape. Int J Comp Vision 2007;72:195–215.

Duan Q, Angelini E, Gerard O, Costa KD, Holmes JW, Homma S, Laine A. Cardiac motion analysis based on optical flow on real-time 3D ultrasound data. In: Suri JS, Fenster A, Chang R-F, et al., eds. Recent Advances in Diagnostic and Therapeutic 3-D Ultrasound Imaging for Medical Applications. Artech House, Inc., 2007a.

Duan Q, Shechter G, Gutierrez LF, Stanton D, Zagorchev L, Laine AF, Daniel Elgort. Augmenting CT cardiac roadmaps with segmented streaming ultrasound. SPIE Int Symp Med Imaging 2007. San Diego, California. 2007b:65090V1–65090V11.

Duan Q, Angelini E, Gerard O, Homma S, Laine A. Comparing optical-flow based methods for quantification of myocardial deformations on RT3D ultrasound. IEEE Int Symp Biomed Imaging 2006:173–176.

Duan Q, Angelini E, Herz SL, Ingrassia CM, Gerard O, Costa KD, Holmes JW, Homma S, Laine A. Dynamic cardiac information from optical flow using four dimensional ultrasound. 27th Annual International Conference IEEE Engineering in Medicine and Biology Society (EMBS). Shanghai, China, 2005a.

Duan Q, Angelini ED, Herz SL, Gerard O, Allain P, Ingrassia CM, Costa KD, Holmes JW, Homma S, Laine AF. Tracking of LV endocardial surface on real-time three-dimensional ultrasound with optical flow. Third International Conference on Functional Imaging and Modeling of the Heart 2005. Barcelona, Spain 2005b:434–445.

Duan Q, Angelini ED, Laine A. Assessment of visual quality and spatial accuracy of fast anisotropic diffusion and scan conversion algorithms for real-time three-dimensional spherical ultrasound. SPIE Int Symp Med Imaging. San Diego, California. 2004:331–342.

Fenster A, Downey DB. Three-dimensional ultrasound imaging, In: Jacob Beutel HLK, Metter RL, eds. Handbook of Medical Imaging Volume1 Physics and Psychophysics. Bellingham, WA: SPIE- The International Society of Optical Engineering, 2000:463–510.

Frangi AF, Niessen WJ, Viergever MA. Three-dimensional modeling for functional analysis of cardiac images, a review. IEEE Trans Med Imaging 2001;20:2–25.

Heijman E, Aben J-P, Penners C, Niessen P, Guillaume R, Eys Gv, Nicolay K, Strijkers GJ. Evaluation of manual and automatic segmentation of the mouse heart from CINE MR images. J Magn Reson Imaging 2008;27:86–93.

Herz S, Ingrassia C, Homma S, Costa K, Holmes J. Parameterization of left ventricular wall motion for detection of regional ischemia. Ann Biomed Eng 2005;33:912–919.

Horn BKP, Schunck BG. Determing optical flow. Artificial Intel 1981; 17:185–203.

Horstman JA, Monaghan MJ, Gill EA. Intraventricular dyssynchrony assessment by real-time three-dimensional echocardiography. Cardiol Clin 2007;25:253–260.

Hunter PJ, Smaill BH. The analysis of cardiac function: A continuum approach. Progr Biophys Mol Biol 1988;52:101–164.

Ingrassia C, Usyk T, Kerckhoffs R, McCulloch A, Costa K, Holmes J. Model-based development of 4-dimensional wall motion measures. Comp Meth Appl Mech Eng 2007;196:3061–3069.

Ingrassia CM, Herz SL, Costa KD, Holmes JW. Impact of ischemic region size on regional wall motion. Proceedings of the 2003 Annual Fall Meeting of the Biomedical Engineering Society, 2003.

Juergens KU, Seifarth H, Range F, Wienbeck S, Wenker M, Heindel W, Fischbach R. Automated threshold-based 3D segmentation versus short-axis planimetry for assessment of global left ventricular function with dual-source MDCT. Am J Roentgenol 2008;190: 308–314.

Kapetanakis S, Kearney M, Siva A, Gall N, Cooklin M, Monaghan M. Real-time three-dimensional echocardiography: A novel technique to quantify global left ventricular mechanical dyssynchrony. Circulation 2005;112:992–1000.

Ledesma-Carbayo MJ, Kybic J, Desco M, Santos A, Sühling M, Hunziker P, Unser M. Spatio-temporal nonrigid registration for ultrasound cardiac motion estimation. IEEE Trans Med Imaging 2005;24:1113–1126.

Linguraru MG, Vasilyev NV, Nido PJd, Howe RD. Atrial septal defect tracking in 3D cardiac ultrasound. Lecture Notes Comp Sci 2006; 4190:596–603.

Lucas B, Kanade T. An iterative image registration technique with an application to stereo vision. Proc DARPA IU Workshop 1981a.

Lucas BD, Kanade T. An iterative image registration technique with an application to stereo vision. International Joint Conference on Artificial Intelligence (IJCAI) 1981b:674–679.

Mikic I, Krucinski S, Thomas JD. Segmentation and tracking in echocardiographic sequences: Active contours guided by optical flow estimates. IEEE Trans Med Imaging 1998;17:274–284.

Montagnat J, Sermesant M, Delingette H. Anisotropic filtering for model-based segmentation of 4D cylindrical echocardiographic images. Pattern Recogn Lett 2003;24:815–828.

Nagel H. Displacement vectors derived from second-order intensity variations in image sequences. Comp Vision Graphics Image Proc 1983;21:85–117.

Ofili EO, Nanda NC. Three-dimensional and four-dimensional echocardiography. Ultrasound Med Biol 1994;20:00.

Paragios N. A level set approach for shape-driven segmentation and tracking of the left ventricle. IEEE Trans Med Imaging 2003;22: 773–776.

Pednekar A, Kakadiaris IA, Kurkure U, Muthupillai R, Flamm S. Validation of the automatic computation of the ejection fraction from cine-MRI. Lecture Notes Comp Sci 2003;2879:987–989.

Perona P, Malik J. Scale space and edge detection using anisotropic diffusion. IEEE Workshop on Computer Vision 1987:16–22.

Perona P, Malik J. Scale-space and edge detection using anisotropic diffusion. IEEE Trans Pattern Anal Machine Intell 1990;12:629–639.

Ramm OTV, Smith SW. Real time volumetric ultrasound imaging system. J Digital Imaging 1990;3:261–266.

Rankin RN, Fenster A, Downey DB, Munk PL, Levin MF, Vellet AD. Three-dimensional sonographic reconstruction: Technique and diagnostic applications. Am J Radiol 1993;161:695–702.

Revell J, Mirmehdi M, McNally D. Combined ultrasound speckle pattern similarity measures. Med Image Understanding Anal 2004: 149–53.

Sanchez-Ortiz GI, Wright GJT, Clarke N, Declerck J, Banning AP, Noble JA. Automated 3-D echocardiography analysis compared with manual delineations and SPECT MUGA. IEEE Trans Med Imaging 2002;21:1069–1076.

Singh A. An estimation-theoretic framework for image-flow computation. Int Conf Comp Vision 1990.

Suhling M, Arigovindan M, Jansen C, Hunziker P, Unser M. Myocardial motion analysis from B-mode echocardiograms. IEEE Trans Image Proc 2005;14:525–536.

Tsuruoka S, Umehara M, Kimura F, Wakabayashi T, Miyake Y, Sekioka K. Regional wall motion tracking system for high-frame rate ultrasound echocardiography. Proceedings of the 1996 4th International Workshop on Advanced Motion Control, AMC'96. Part 1. Tsu, Japan. IEEE 1996:389–394.

van Geuns RJM, Baks T, Gronenschild EHBM, Aben J-PMM, Wielopolski PA, Cademartiri F, de Feyter PJ. Automatic quantitative left ventricular analysis of cine MR images by using three-dimensional information for contour detection. Radiology 2006; 240:215–221.

Veronesi F, Corsi C, Caiani EG, Sarti A, Lamberti C. Tracking of left ventricular long axis from real-time three-dimensional echocardiography using optical flow techniques. IEEE Trans Informat Technol Biomed 2006;10:174–181.

Voormolen MM, Krenning BJ, Lancee CT, Cate FJt, Roelandt JRTC, Steen AFW, Jong ND. Harmonie 3-D echocardiography with a fast-rotating ultrasound transducer. IEEE Trans Ultrason Ferroelectr Freq Control 2006;53:1739–1747.

Wang T, Gu IYH, Viberg M, Cao Z, Song N. Tracking moving objects in video using enhanced mean shift and region-based motion field. EUSIPCO 2007:307–311.

Weickert J, Romeny BMtH, Viergever MA. Efficient and reliable schemes for nonlinear diffusion filtering. IEEE Trans Image Proc 1998;7:398–410.

Xiao J, Zhang Y, Shah M. Adaptive region-based video registration. Motion and Video Computing 2005.

Yilmaz A, Javed O, Shah M. Object tracking: A survey. ACM Comp Surveys 2006;38:1–-45.

Yu W, Lin N, Yan P, Purushothaman K, Sinusas A, Thiele K, Duncan JS. Motion Analysis of 3D ultrasound texture patterns. Lecture Notes Comp Sci 2003;edn 2674;252–261.

Yu W, Yan P, Sinusas AJ, Thiele K, Duncan JS. Towards pointwise motion tracking in echocardiographic image sequences: Comparing the reliability of different features for speckle tracking. Med Image Anal 2006;10:495–508.